*Atmósfera(1997), **11**, pp. 239-256*

Effects of roughness length on the FSU one-dimensional atmospheric boundary layer model forecasts

A. BIROL KARA, AHSHA TRIBBLE and PAUL H. RUSCHER

Department of Meteorology, The Florida State University, Tallahassee, FL, 32306-4520, USA

(Manuscript received August 12, 1997; accepted in final form May 11, 1998)

RESUMEN

Este trabajo se ocupa de la sensibilidad de los pronósticos obtenidos con el "Modelo de la capa fronteriza de la Universidad Estatal de Florida (FSU1DPBL)", cuando se considera exclusivamente una variación en el parámetro de la longitud de rugosidad. El modelo se usa principalmente para evaluar la sensibilidad de la longitud de rugosidad del momentum en los pronósticos del modelo. Los cálculos de la longitud de rugosidad se llevan a cabo usando ambas, las componentes del viento y la dirección del mismo. Con base en estos modelos, los valores comunes de la longitud de rugosidad de momentum, indicados en la literatura, se comparan con los de Tallahassee (TLH) calculados a partir de las observaciones. Además, los pronósticos del modelo obtenidos usando esta longitud de rugosidad se comparan con los obtenidos usando el valor clásico de la longitud de rugosidad. El enfoque en estas comparaciones reside principalmente en las variaciones, si acaso existen en los pronósticos de la altura de la capa atmosférica fronteriza (ABL), flujos de calor sensible y del latente y la velocidad del viento a 10 m. Los resultados muestran que los flujos no tienen mucha variación cuando se usa, ya sea la longitud de rugosidad clásica o la longitud de rugosidad calculada. Sin embargo, la velocidad del viento a 10 m parece ser sobreestimada, usando el valor clásico de la longitud de rugosidad, en comparación con el valor calculado.

ABSTRACT

This paper is concerned with the sensitivity of the forecasts obtained from the "Florida State University Atmospheric Boundary Layer (FSU1DPBL) Model" when solely considering a variation in the roughness length parameter. The model is mainly used to evaluate the sensitivity of the roughness length of momentum on the model forecasts. The roughness length calculations are perfomed using both wind speed components and wind direction. Based on these calculations, the commonly used values of roughness length of momentum indicated in the literature is compared to that for Tallahassee (TLH) calculated from observations. In addition, model forecasts obtained using the calculated roughness length are compared with those using the classical value of the roughness length. The focus on these comparisons is mainly on the variations, if any, in the forecasts for the atmospheric boundary layer (ABL) height, sensible heat flux, soil heat flux, latent heat flux, and 10-meter wind speed. Results show that the fluxes do not have much variation when using both classical roughness length and the calculated roughness length. However, the 10-meter wind speed appears to be overestimated using the classical roughness length value in comparison to the calculated value.

1. Introduction

The surface heat fluxes (sensible, latent and soil fluxes) are of crucial importance in modeling studies pertaining to the atmospheric boundary layer (Troen and Mahrt, 1986; Holtslag and Ek, 1996). The reason is that they determine the mean profiles of the surface layer and atmospheric boundary layer (ABL). The lower ABL is mostly affected by turbulence while the upper layer is affected by clear air radiative cooling at night (André and Mahrt, 1982). Modeling studies have attempted to parameterize the surface fluxes of heat, momentum and moisture. Different approaches have been taken to forecast boundary layer parameters such as temperature, boundary layer depth and stability. In many of these models, the atmospheric boundary layer is treated either by eddy diffusivity (K theory) or by mixed layer models (O'Brien, 1970; Nieuwstadt and Driedonks, 1979).

Surface fluxes depend on many parameters such as vegetation, soil type, soil moisture and stability-dependent coefficients which involve roughness lengths of heat momentum. Therefore, the roughness length is an essential parameter to determine surface heat fluxes. The roughness is best characterized by the roughness length which can be obtained from the relative change of average wind speed with height in neutral stability at levels above the roughness elements (Beljaars and Holtslag, 1991; Wieringa, 1992). In the model used in this study the vegetation system is very sensitive to the ratio of the roughness lengths (Kara *et al.*, 1998). This ratio is described as $\frac{Z_{OM}}{Z_{OH}}$ where Z_{OM} is the roughness length of momentum, and Z_{OM} is the roughness length of heat (Stull, 1983). In the FSU1DPBL the best agreement for the ABL parameters can be obtained by using a roughness length of heat which is three order of magnitude smaller than that of momentum over heterogeneous vegetation (Holtslag and Ek, 1996).

An increased roughness parameter together with an increased displacement height can result in a decrease in the wind speed and; thereby, a decrease in the ABL height (h). Zhang and Anthes (1982) showed that the heat flux is reduced due to stronger evaporation as the roughness length increases. The increased evaporation and reduced depth of the ABL associated with a large roughness length increases the low level moisture. Garratt and Pielke (1989) found that mean profiles of the ABL were not very sensitive to the roughness length at night by using a one-dimensional ABL model. Their results were relatively insensitive to changes in the surface layer parameterization constants. On the other hand, in a previous study, Kara *et al.* (1998) showed that the one-dimensional ABL (FSU1DPBL) model is very sensitive to the roughness length value used for a near coastal location. We examine this sensitivity in detail in this investigation.

2. Data description

The Tallahassee Regional Airport (TLH) is located in the central Panhandle of northern Florida. It is approximately 35 km inland of the Gulf of Mexico coast (Fig. 1). In our analysis a 5-minute interval of wind speed (u, v components and total wind speed, V) and wind direction as obtained from the TLH airport between October 17, 1996 and October 29, 1996 are used to determine roughness length at the TLH airport. In the model forecasts 12 hourly upper-air sounding from the airport is used as will be explained later. For the purpose of calculating the roughness length, only the wind speed/direction data from 1700 LST (Local Standard Time) and 2000 LST were used. This is done to ensure that the data set used would represent near-neutral conditions - a condition needed to apply various scaling techniques when estimating an effective roughness length, Z_{OM}, as explained by Beljaars and Holtslag (1991). Figure 2 illustrates a time series of total wind speed and its corresponding u and v components for the 12-day period mentioned above. Also included are the class intervals for the total wind speed and 30 degree class intervals for the wind direction (Fig. 3). The mean of v wind component of the wind speed is greater than that of u wind component indicating that the dominating wind flow is in the north-south direction at the airport.

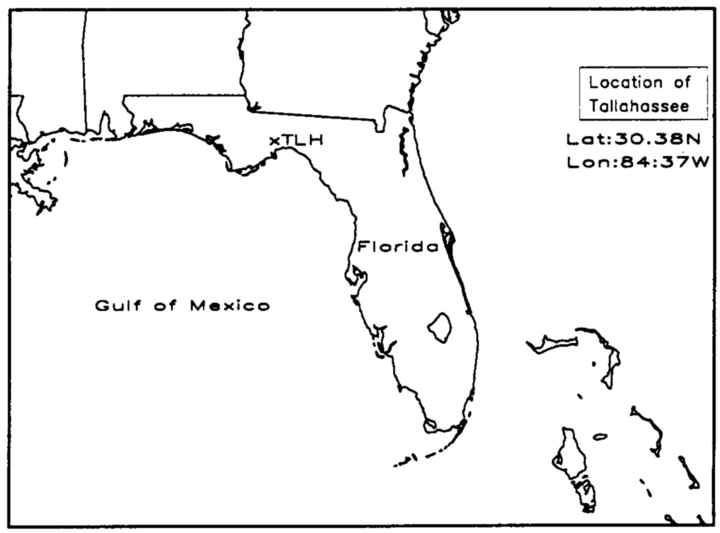

Fig. 1. The location of the Tallahassee regional airport (TLH) in the southeastern United States. The latitude and longitude of TLH are also written in upper right corner.

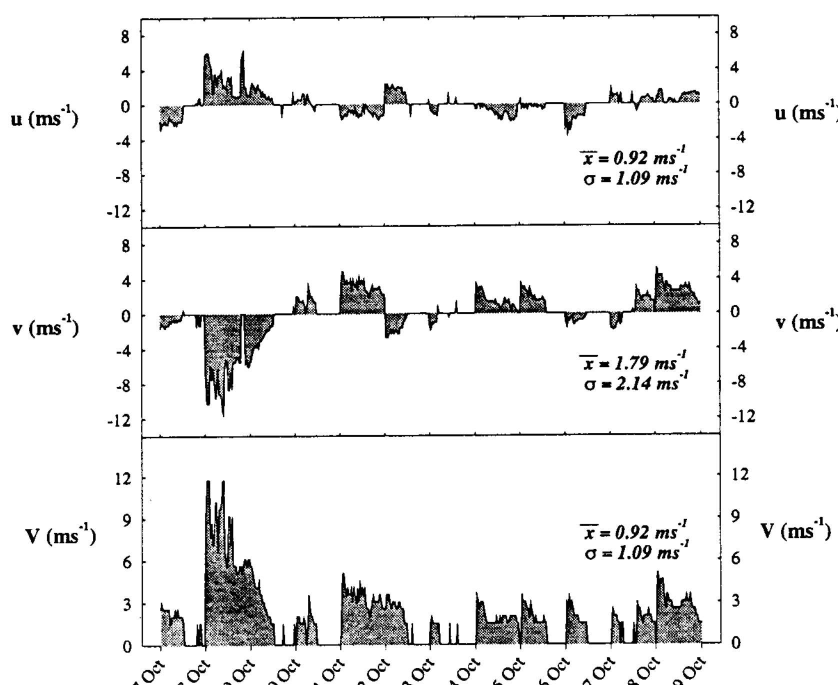

Fig. 2. The horizontal (u and v) components of the wind speed and the total wind speed (V) obtained from TLH regional airport from October 17, 1996 to October 29, 1996 between 1700 LST (Local Standard Time) and 2000 LST. Also included are the mean ($\overline{x}$) and standard deviation (σ) of each variable.

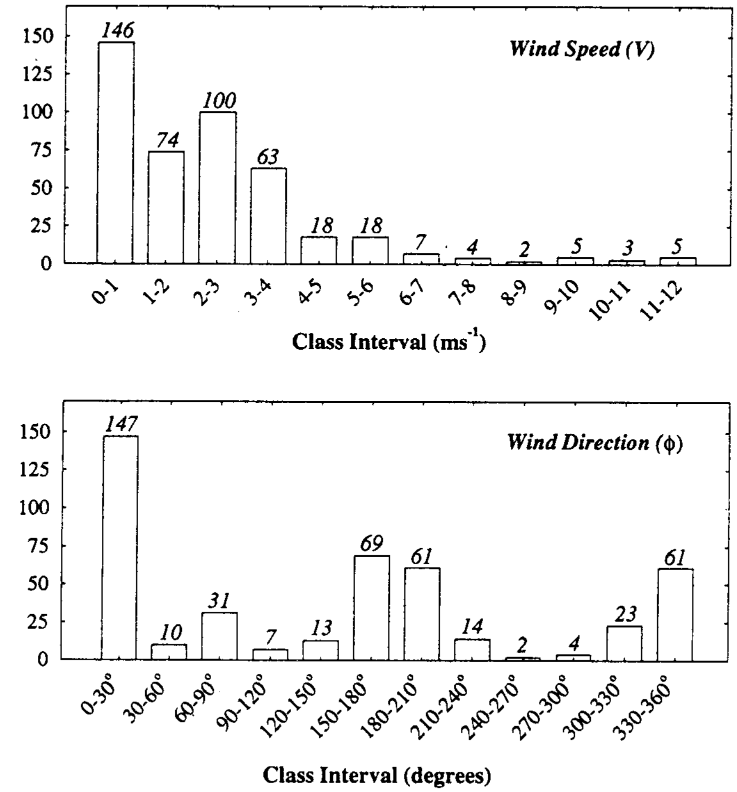

Fig. 3. Class intervals for the total wind speed (V), and the 30° class intervals for the wind direction from the same data set used in Figure 2.

3. Boundary layer parameterizations

The ABL model used here is described with eddy-diffusivity (K-theory) and counter-gradient transport terms (Troen and Mahrt, 1986). The ABL model is coupled with an active two-layer soil model and a primitive plant canopy model (Mahrt and Pan, 1984; Pan and Mahrt, 1987). In the following section we summarize the equations used in the models. Further information about the model may also be found in Kara (1996a) and Kara (1996b).

a. *Model equations*

Horizontal components of the wind V_h (u and v components), potential temperature (θ), and specific humidity (q) are calculated as follows:

$$\frac{\partial V_h}{\partial t} = \frac{\partial}{\partial z}\left(K_m \frac{\partial V_h}{\partial z}\right) - w\frac{\partial V_h}{\partial z}, \tag{1}$$

$$\frac{\partial \theta}{\partial t} = \frac{\partial}{\partial z}\left[K_h \left(\frac{\partial \theta}{\partial z} - \gamma_\theta\right)\right] - w\frac{\partial \theta}{\partial z}, \tag{2}$$

$$\frac{\partial q}{\partial t} = \frac{\partial}{\partial z}\left(K_h \frac{\partial q}{\partial z}\right) - w\frac{\partial q}{\partial z}, \tag{3}$$

where, K_m and K_h are the eddy diffusivities for momentum and heat, respectively, and γ_θ is the counter gradient correction for potential temperature as will be explained below. Only the vertical diffusion terms due to boundary layer mixing and the vertical advection terms due to a prescribed vertical motion are considered in order to evaluate these equations. In the model V_h, θ and q are calculated at the computational levels; while their vertical derivatives, $\partial V_h/\partial z$, $\partial\theta/\partial z$ and $\partial q/\partial z$, are calculated between computational levels. The vertical velocity, w, is estimated using the method of O'Brien (1970), which is a correction to the traditional kinematic method.

The counter gradient correction term γ_θ in Eq. 1 for potential temperature represents non-local influences on mixing by turbulence (Deardorff, 1972). Since transport of heat by turbulent eddies can be assumed small at night, this correction term is neglected for stable conditions. The term γ_θ is evaluated in terms of surface flux of potential temperature $(\overline{w'\theta'})_s$, the boundary layer depth (h), and a nondimensional constant (C) which is taken as 8.5 following Holtslag (1987) as follows:

$$\gamma_\theta = \begin{cases} 0 & \text{for stable cases,} \\ C\frac{(\overline{w'\theta'})_s}{w_s h} & \text{for unstable cases,} \end{cases} \tag{4}$$

where, w_s is the velocity scale of the ABL, and z_s is the top of the surface layer ($0.1h$ in the model). The velocity scale is parameterized as follows:

$$w_s = u_*(\Phi_m)^{-1}\left(\frac{z_s}{L}\right), \tag{5}$$

where, u_* and L denote the surface friction velocity and *Monin-Obukhov length*, respectively. The non-dimensional profile functions (Φ) for the shear and temperature gradients are taken from Businger *et al.* (1971) with modifications by Holtslag (1987), and they are functions of height (z) and length (L).

b. Surface layer model

The surface fluxes are parameterized following Mahrt (1987) for the stable case and following Louis *et al.* (1982) for the unstable case as

$$u_*^2 = C_m(V_o), \tag{6}$$

$$(\overline{w'\theta'})_s = C_h(\theta_s - \theta_o), \tag{7}$$

$$(\overline{w'q'})_s = C_h(q_s - q_o), \tag{8}$$

where, C_m and C_h are the stability-dependent exchange coefficients defined as functions of the roughness length of heat (Z_{0H}) and momentum (Z_{0M}). Here (V_o) is the wind speed evaluated at the first model level (60 m for the stable case) above the surface. The surface fluxes are influenced by the interaction of the vegetated surface over land. The surface ABL parameterizations of the model allow for a distinction between direct evaporation from the soil and transpiration by the vegetation. Thus, we should expect some variation of these fluxes when the roughness length is changed.

As shown above, surface heat fluxes in the model depend on the roughness length for momentum, Z_{0M}, used in the model. To understand the relationship between the roughness length and surface fluxes, we first introduce the variables C_m and C_h (the exchange coefficients for momentum and heat) used in the model, respectively.

$$C_m = k^2 \mid V_o \mid \frac{F1(Z, Z_{0M}, Ri_B)}{(\ln \frac{Z}{Z_o})^2}, \tag{9}$$

$$C_h = \frac{k^2}{R} \mid V_o \mid \frac{F2(Z, Z_{0M}, Z_{0H}, Ri_B)}{(\ln \frac{Z}{Z_o})(\ln \frac{Z}{Z_{0H}})}, \tag{10}$$

where, k is the nondimensional *von Kármán* constant ($k = 0.4$), and R, estimated at 1.0, is the ratio of the drag coefficients for momentum and heat in the neutral limit and is taken from Businger *et al.* (1971) with some modifications. As seen, C_m and C_h are functions of the wind speed evaluated at the first model level above the surface ($\mid V_o \mid$), the height of the first model layer above the surface (Z), the roughness length for momentum (Z_{0M}) depending on surface characteristics and the bulk Richardson number (Ri_B) for the surface layer.

The functions $F1$ and $F2$ used in Eqs. 9 and 10 are defined as follows:

$$F1 = \left\{ \begin{array}{ll} e^{-aRi_B} & \text{for stable cases,} \\ 1 - \dfrac{10Ri_B}{1+7.5\left[\dfrac{k^2}{\left(\ln \frac{Z}{Z_{0M}}\right)^{1/2}}10\right]\left[-Ri_B \frac{Z}{Z_{0M}}\right]^{1/2}} & \text{for unestable cases,} \end{array} \right\}$$

$$F2 = \left\{ \begin{array}{ll} e^{-aRi_B} & \text{for stable cases,} \\ 1 - \dfrac{15Ri_B}{1+7.5\left[\dfrac{k^2}{\left(\ln \frac{Z}{Z_{0M}}\right)\left(\ln \frac{Z}{Z_{0H}}\right)}10\right]\left[-Ri_B \frac{Z}{Z_{0M}}\right]^{1/2}} & \text{for unestable cases,} \end{array} \right\}$$

where, a is a constant currently equal to 1.0 in the model.

The length scale for the surface layer is the *Monin-Obukhov length*, and it is described as

$$L = -\frac{\theta_{sv};u_*^3}{gk(\overline{w'\theta'})_s}, \tag{11}$$

where the surface virtual potential temperature is denoted as (θ_{sv}), g is the gravitational acceleration ($g = 9.8$ m s^{-2}) and k is the *von Kármán* constant taken as 0.4 in the model as indicated before. *Monin-Obukhov length* is used in the non-dimensional profile functions. The only variables needed to close the surface layer model are q_s and θ_s, which are available from the soil model and the surface energy balance calculation, respectively. The surface specific humidity (q_s) is calculated as follows:

$$q_s = q_o + \frac{E}{\rho_o C_h}, \tag{12}$$

where, q_o is the specific humidity at the air-soil interface ($z = 0$) at the first model level, E is the total evaporation, and ρ_o is the air density at the surface. Further information about the soil model can be found in Mahrt and Pan (1984) and Pan and Mahrt (1987).

The surface energy balance is given as follows:

$$\underbrace{(1-\alpha)S\downarrow}_{Term\ 1} + \underbrace{L\downarrow}_{Term\ 2} - \underbrace{\sigma\theta_s^4\uparrow}_{Term\ 3} = \underbrace{G\downarrow}_{Term\ 4} + \underbrace{H\uparrow}_{Term\ 5} + \underbrace{L\times E\uparrow}_{Term\ 6}, \tag{13}$$

where each term is expressed in Watts per square meter ($\mathrm{Wm^{-2}}$).

Term 1: Downward solar radiation. The non-dimensional coefficient α is the surface albedo.

Term 2: Downward atmospheric radiation.

Term 3: Upward terrestrial radiation. σ is the *Stefan-Boltzmann* constant (5.7×10^{-8} $\mathrm{Wm^{-2}}$ $\mathrm{K^{-4}}$).

Term 4: Downward soil heat flux.

Term 5: Upward sensible heat flux. It is defined as

$$H = \rho_o C_p C_h(\theta_s - \theta_o), \tag{14}$$

and is a function of the air density (ρ_o), the specific heat (C_p) that is 1004.5 J $\mathrm{kg^{-1}}$ $\mathrm{K^{-1}}$ for air, a stability-dependent exchange coefficient (C_h) and the difference between the surface temperature (θ_s) and the air potential temperature at the first model level (θ_o).

Term 6: Upward latent heat flux where $L = 2.5 \times 10^6$ J $\mathrm{kg^{-1}}$ is the latent heat of vaporization. Total evaporation (E) is obtained by adding the direct soil evaporation, the transpiration and the canopy evaporation (Mahrt and Pan, 1984).

The surface energy balance is solved to derive an effective radiative (skin) surface temperature as indicated in Pan and Mahrt (1987). Incoming atmospheric longwave radiation is parameterized according to Satterlund (1979), and the incoming solar radiation is calculated following the method of Kasten and Czeplak (1980). The model predicts cloud cover using the generalized equation, $CLC = f(\overline{RH}, \sigma_{RH})$, where CLC is the fractional cloud cover, $\overline{RH}$ is the maximum relative humidity in the boundary layer, and σ_{RH} is the standard deviation of relative humidity accounting for the turbulent and subgrid mesoscale variations in relative humidity.

c. ABL Height

The ABL height is defined as the height at which turbulent transfers of heat, momentum and mass are significant. We use the definition of Troen and Mahrt (1986) where the transition between a stable and an unstable case is continuous to determine the ABL height (h) as shown below:

$$h = \frac{Ri_{cr}\theta_{ov}[V(h)]^2}{g[\theta_v(h) - \theta^*_{ov}]}, \tag{15}$$

where, Ri_{cr} is the critical Richardson number (0.5 in the model), θ_{ov} is the reference virtual potential temperature at the first model level above the surface, V_h is the horizontal wind velocity at level h. This approach to diagnosing the h also requires the specification of a low-level potential temperature (θ^*_{ov}). This low-level potential temperature can be expressed as,

$$\theta^*_{ov} = \begin{cases} \theta_{ov} & \text{for stable cases,} \\ \theta_{ov} + C\frac{\overline{(w'\theta')_s}}{w_s} & \text{for unstable cases.} \end{cases} \tag{16}$$

Examination of Eq. (15) indicates that h can be calculated for all stability conditions when the surface fluxes and profiles of θ_v and V_h are known.

d. Model Initialization

The initial vertical profiles of horizontal wind, potential temperature and mixing ratio are determined from the appropriate operational sounding at the TLH airport. All mandatory and significant data levels are utilized. After this process, data are interpolated to the model vertical grid, which has layers, with 80 m vertical resolution near the surface and extending up to the free atmosphere. Several parameters must be input to the model to perform a forecast. The

Table 1: The parameters used for the model initialization. The unit, if exists, is also given for each parameter. Each model forecast was initialized with the same parameters except roughness length.

Parameters for the model initialization	Value
Roughness length for momentum (m)	0.01, 0.0441
Roughness length for heat (m)	0.01
Displacement height of vegetation (m)	0.00
Albedo	0.23
Soil type	Sandy clay
Shading factor	0.00
Air dry value	0.07
Transpiration reduction reference value	0.25
Plant coefficient	0.00
Soil moisture (%)	30
U_g (geostrophic wind component (m s^{-1})	0.30
V_g (geostrophic wind component (m s^{-1})	2.00

site considered in this study has different surface properties. The parameters used in the model initialization for all forecasts performed are shown in Table 1. The albedo value of 0.23 was obtained from Stull (1983). The soil type, sandy clay, was obtained from the "U. S. Department of Agriculture Soil Survey Maps", and the soil moisture used was 30% (Kara, 1996b). For sandy clay, the wilting factor is 0.18 (Clapp and Hornberger, 1978).

For the model initialization, a proper choice of roughness length is necessary since surface layer parameterization is sensitive to these values. In many models the roughness lengths are often taken equal to each other (i.e., $Z_{OH} = Z_{OM}$); although, roughness length for momentum Z_{OM} is at least one order larger than the one for heat Z_{OH} over homogeneous vegetated surfaces (Garratt, 1978; Brutsaert, 1982). The ratio, $\frac{Z_{OM}}{Z_{OH}}$, was found to be approximately 12 for that kind of vegetation area. Also Arya (1975) indicated that tall trees have large effects on the vertical momentum transfer; however, we do not have such a vegetation at TLH airport.

4. Roughness length determination

To gain an understanding of the overall transfer between the ABL and the underlying surface it is necessary to determine several parameters such as sensible heat flux, wind speed and ABL height. For vertical momentum transfer, the level at which the wind speed becomes zero on extrapolation of the wind profile is described by the parameter $(d + Z_O)$ where d, displacement height, is taken to be zero since the TLH regional airport is characterized by short grass.

The roughness length calculation performed here is based on the method used by Beljaars and Holtslag (1991). They actually compute what is called an "effective roughness length". Obtaining this value from an empirical table, relating roughness lengths to different types of surface cover is usually inaccurate. It is appropriate to calculate an effective roughness length which will yield the correct area-averaged momentum flux in a model. Throughout the paper, then, the calculated, effective roughness length will be referred to simply as just roughness length or Z_{OM} for ease of notation. Since we use wind speed components (u and v) just after sunset at the TLH airport, we can assume near-neutral conditions, i.e., the boundary layer height divided by the *Monin-Obukhov length* is sufficiently small. Thus, we can apply the following scaling relations as given by Beljaars and Holtslag (1991):

$$\frac{\sigma_u}{u_*} = 2.2, \quad \frac{\sigma_v}{u_*} = 1.9, \quad \sigma_v = U\sigma_\phi, \tag{17}$$

$$\frac{V}{u_*} = \left(\frac{1}{k}\right) \ln\left(\frac{Z}{Z_{OM}}\right). \tag{18}$$

Combining (17) and (18), we get Z_{OM},

$$2.2\left(\frac{V}{\sigma_u}\right) = \left(\frac{1}{k}\right) \ln\left(\frac{Z}{Z_{OM_u}}\right), \tag{19}$$

$$1.9\left(\frac{V}{\sigma_v}\right) = \left(\frac{1}{k}\right) \ln\left(\frac{Z}{Z_{OM_v}}\right), \tag{20}$$

where, $V = \sqrt{\overline{u}^{\,2} + \overline{v}^{\,2}}$ and $\overline{u}$ and $\overline{v}$ are the mean horizontal components of the wind speed within a specific wind direction class interval. In these equations k is taken as 0.4 as mentioned before, and Z has a value of 10 m. Here it should be noted that Z_{0M} is calculated for u and v components, separately.

At this point Beljaars and Holtslag (1991) suggest we look at peak winds or gusts; thereby, eliminating u, $v \leq 2$ ms^{-1}, and separate the remaining winds into a 30-degree class intervals. Since the current sample data size we have is relatively small, a 60-degree wind direction interval is used for the calculations of the mean ($\overline{u}$, $\overline{v}$) and standard deviations (σ_u, σ_v) of the wind speed components, respectively (Table 2). Once $\overline{u}$, $\overline{v}$, σ_u, and σ_v are obtained, the computation of the roughness lengths are possible using Eqs. (19) and (20). The results are illustrated in Table 3.

Table 2: The mean ($\overline{u}$, $\overline{v}$) and standard deviation (σ_u, σ_v) of horizontal wind components of the wind speed, and the t-values are shown for each 60° interval. The data set is from October 17, 1996 to October 26, 1996 from 1700 UTC to 2000 UTC with $v \leq 2$ m s^{-1} removed. The number of observations (n) is also written.

Wind Direction (degree)	n	$\overline{u}$ (m s^{-1})	σ_u (m s^{-1})	n	$\overline{v}$ (m s^{-1})	σ_v (m s^{-1})
0-60	6	1.63	0.49	6	1.59	0.23
60-120	18	2.32	0.49	18	0.71	0.20
120-180	45	0.94	0.41	45	3.01	0.84
180-240	36	0.87	0.37	36	2.79	0.90
240-300	0	.	.	0	.	.
300-360	53	2.06	1.07	53	5.07	2.83

Table 3: The roughness lengths calculated by using u and v wind components, (Z_{OM_u}) and (Z_{OM_v}), respectively. The calculations are given for each 60° interval of wind direction. The calculated $t-values$ are in parentheses. The arrows indicate the accepted roughness length values according to a 95 % confidence interval by using the "Null hypothesis".

Wind Direction (ϕ) (degree)	Z_{OM_u} ($t-value$) (m)	Z_{OM_v} ($t-value$) (m)
0-60	0.1675 (0.73)	0.0011 (-4.89) ←
60-120	0.1282 (0.32)	0.0010 (-2.14) ←
120-180	0.0115 (-7.06) ←	0.5769 (-2.90) ←
180-240	0.0096 (2.99) ←	0.8480 (0.32)
240-300	0.0000 (0.00)	0.0000 (0.00)
300-360	0.1112 (-4.69) ←	2.3000 (1.09)

The calculated t-values are also used to test the significance of the correlation coefficients between the wind speed and its corresponding roughness length. According to the ***student t-distribution***, the values accepted are those outside of the $\pm$ 1.96 for 95% confidence interval. These values are shown in Figure 4. The accepted u-values and v-values are averaged separately giving, $\overline{Z}_{OM_u}$ = 0.0441 m and $\overline{Z}_{OM_v}$ = 0.194 m. In the data set used there were some fairly high wind speed values for the v-component compared to the u-component (see Fig. 2) which played a large role in overestimating the roughness length value (obtained from using the v component) by about one order of magnitude. Therefore, the best choice for the calculated roughness length can be 0.0441 m as opposed to the classical 0.01 m value for TLH. We have yet to prove, however, whether this small change in roughness length will have any significant impact on the model forecasts.

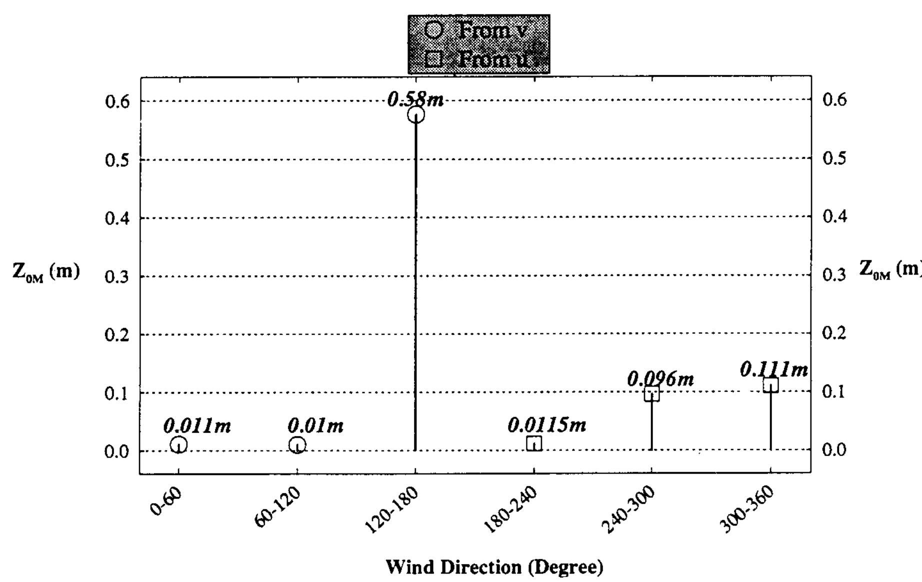

Fig. 4. The roughness length of momentum (Z_{OM}) obtained from u and v wind speed components using 60° wind direction intervals. See text for explanations.

5. Sensitivity to roughness length and error analysis

There were 36 model forecasts performed using the classical roughness length value ($Z_{OM} = 0.01$) and another 36 forecasts performed with that of the calculated roughness length ($Z_{OM} = 0.0441$). In all model forecasts, parameters shown in Table 1 were held constant with the exception of the parameters that will obviously vary day to day; i.e., geostrophic winds. The forecast ABL components analyzed for each roughness length were ABL height (h), sensible heat flux (H), soil heat flux (G), latent heat flux ($L \times E$), and a 10-m wind speed (u and v components).

It is important to recognize, as noted by Murphy (1995), that most of the one-dimensional measures of forecasting performance either focus on one aspect of the quality, such as linear association, or represent a particular composite of many aspects of quality. For the purpose of this study, since we used a dimensional model, a one-dimensional measure of forecasts such as mean-square error and bias is used . Thus, the following equations are used to determine the errors between the model forecasts when using two different roughness lengths.

$$MSE = (\overline{u} - \overline{v})^2 + \sigma_u^2 + \sigma_v^2 - 2\sigma_u\sigma_v r_{uv}, \tag{21}$$

$$\text{Cond. bias} = [r_{uv} - (\frac{\sigma_u}{\sigma_v})]^2, \tag{22}$$

$$\text{Uncond. bias} = [\frac{(\overline{u} - \overline{v})}{\sigma_v}]^2, \tag{23}$$

where, r_{uv} denotes correlation coefficient between u and v components. The results obtained are shown in Table 4. As seen, the values of the mean-square error (MSE) indicate fairly minor discrepancies in the ABL height, sensible heat flux and 10 m wind speed. The difference in h error appears large; but, we must remember that we are dealing with large values of ABL height. Furthermore, it should be noted that we want to be conditionally and unconditionally unbiased, which rarely holds in the real world as seen from Eqs. 22 and 23.

Table 4: The statistical analysis of the 24-hour model forecast comparing Z_{OM} = 0.01 m and Z_{OM} = 0.0441 m (calculated value). The sample size (n), mean-square error (MSE), conditional bias (Cond. Bias), and unconditional bias (Uncond. Bias) are given for each parameter. See text for description of symbols.

Parameters (symbol, unit)	n	MSE	Cond. Bias	Uncond. Bias
ABL height (h, m)	36	649.66	0.00014	0.00001
Sensible heat flux (H, W m^{-2})	36	0.61035	0.00006	0.00005
Latent heat flux ($L \times E$, W m^{-2})	36	0.00073	0.01159	0.00053
Soil heat flux (G, W m^{-2})	36	0.01927	0.00016	0.00045
10 m Wind speed (V, m s^{-1})	36	0.24096	0.03032	0.09406

The model results for two cases, March 3, 1996 and March 13, 1996, are shown in Figure 5. As seen, sensible heat fluxes obtained by using two different roughness length still did not show much variation at all. However, the h did show some changes. Out of the 36 days used, we found there were 17 days ABL had collapsed completely (not shown here). The remaining 19 days contained ABL that did not collapse, 8 of which had nighttime growth. Those 19 cases experienced perturbations in the h profiles, but only at night. Also note that although sensible heat flux did not show any significant variations in its profiles, we found the maximum heat flux was only near 80 W m^{-2} on those 19 cases, as opposed to near 300 W m^{-2} on the days with a collapsed h. The reason might be that the weak surface fluxes probably prevented the h from collapsing in the model. Finally, the 10-m wind speed showed variations in all 36 cases. The overall pattern of the profile was the same, but the calculated roughness length profile had smaller values (Fig. 5).

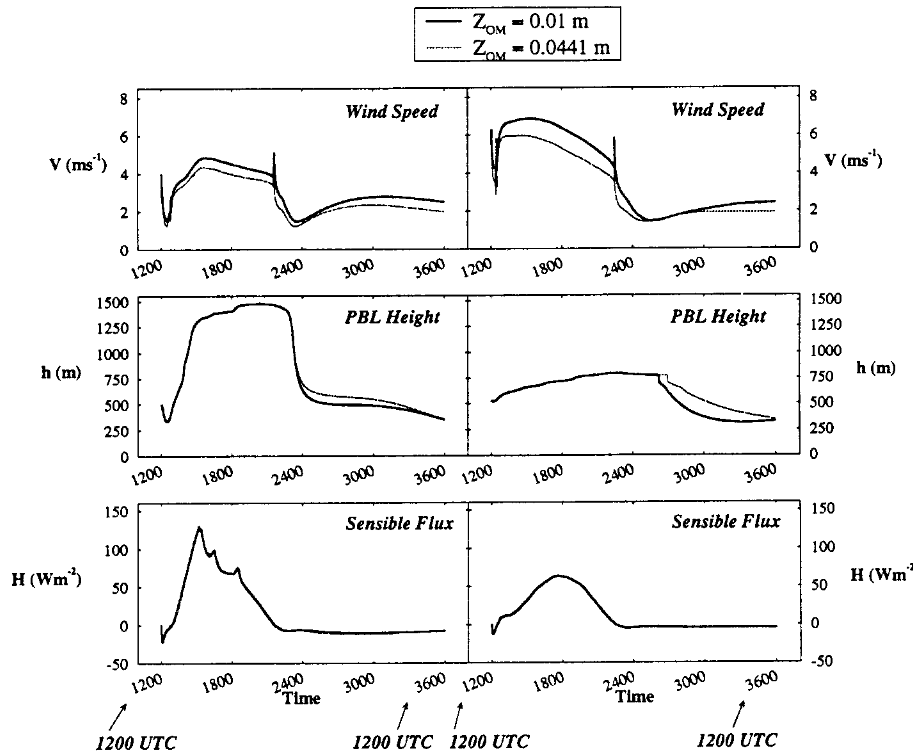

Fig. 5. Forecasts of total wind speed (V), ABL height (h) and sensible heat flux (H) obtained from the model on March 3, 1996 (left column) and March 13, 1996 (right column) with a roughness length of Z_{OM}=0.01 m (solid line) and that of Z_{OM}=0.0441 m (dashed line). The model was initialized at 1200 UTC on both March 3 and 13, 1996 to perform a 24-hr forecast, respectively.

Table 5: The mean ($\overline{x}$) and standard deviation (σ) of the wind speed (V) and ABL height calculated using the differences between these two parameters on 3 and 13 March. This means that the values are obtained from the differences in the forecasts when using the classical roughness length (Z_{OM}=0.01 m) and the calculated roughness length, (Z_{OM}=0.0441 m).

Parameter (symbol, unit)	$\overline{x}$ March 3 (13)	σ March 3 (13)
Total Wind Speed (V, m s^{-1})	3.47 (2.98)	1.66 (1.42)
ABL height (h, m)	454 (529)	115.2 (115.8)

Table 5 shows the mean and standard deviation for the notable differences in the wind speed shown in Figure 5 calculated for the two roughness lengths over the entire period. The standard deviations were quite similar. However, the total mean wind speed when Z_{OM} = 0.01 m was 0.49 m s^{-1} greater than that when Z_{OM} = 0.0441 m. The calculations for the h were made only for the region where the deviation began (nighttime) as shown in Figure 5. The difference

Figures 7 and 8 illustrates the horizontal temperature advection across the southeastern United States for March 3 and March 13, 1996 at 0000 UTC, respectively, 12 hours prior to the model initialization. At the surface, where our focus lies, the magnitude of the temperature advection is less than 1 °C $(\text{day})^{-1}$ on March 3 and less than -1 °C $(\text{day})^{-1}$ on March 13. This implies that horizontal temperature advection is negligible at night. On March 3, the temperature advection at 850 mb and 700 mb is much larger that at the surface but that is above the area of concern. The change in temperature advection with height, shown on the bottom right panel, indicates that the temperature advection increased at 850 mb and tapered off by 700 mb on March 13 over TLH. The change in temperature advection decreases in the low levels which means that there was negligible temperature advection throughout most of boundary layer. This synoptic overview also helps to ensure that the initial conditions are satisfactory to perform a model forecast.

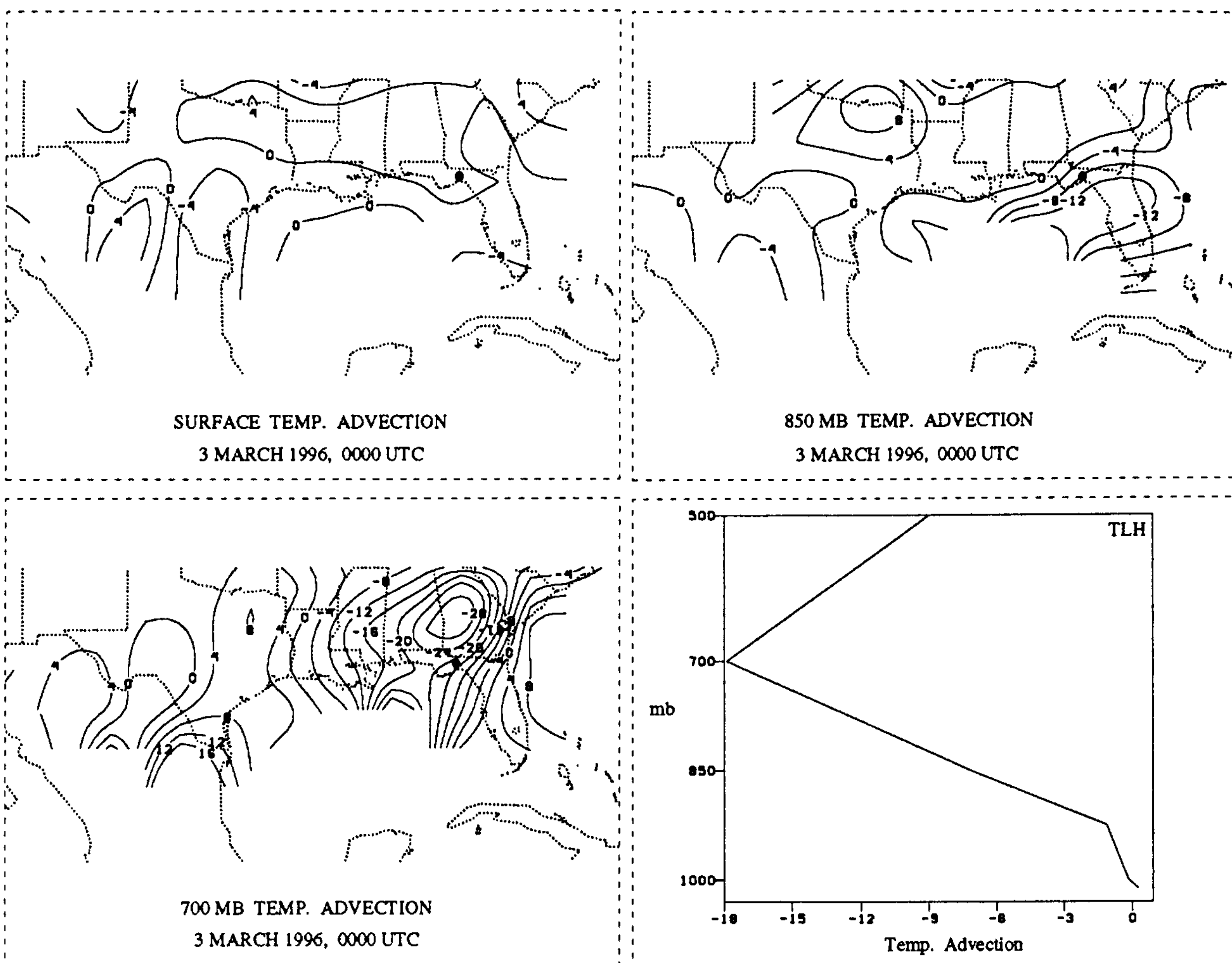

Fig. 7. Observed temperature advection ($^\circ C\ s^{-1} \times 10^{-5}$) at the surface, 850 mb and 700 mb over the southeastern United States for March 3, 1996 at 0000 UTC. The vertical profile of the change in temperature advection (bottom right panel) is also included. The location of TLH is shown with a filled circle (see also Fig. 1)

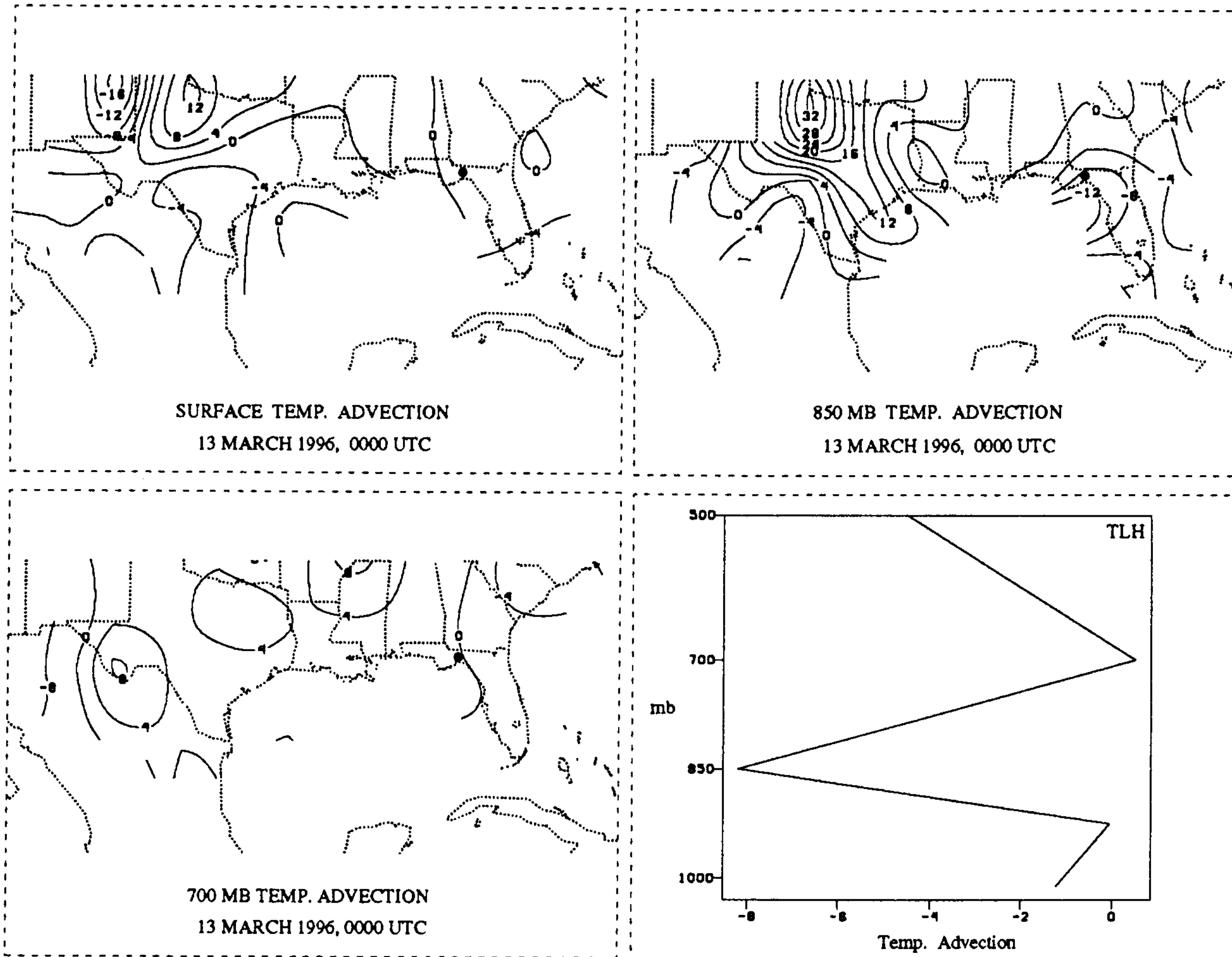

Fig. 8. The same as Figure 7 but for March 13, 1996.

6. Conclusion

The roughness length is an important parameter in atmospheric boundary layer studies. The use of an inaccurate roughness length value can have an adverse effect on model results over coastal locations as well since these locations generally experience more wind variations. We showed that in the model forecasts the use of the roughness length calculated from the observed wind speed gives better results than the use of classical roughness length reported in the literature. Since ABL height calculation in the model used in this study depends on wind speed [Eq. (15)], an over/underestimation of the wind speed will over/underestimate the ABL height. The overestimation could also be linked to the fluctuation in ABL height during night. Thus, the model results are sensitive to a small variations in roughness length, and depending on which parameter you are intending to forecast, there may be considerable differences. This estimate of wind speed depends on the roughness length; therefore, it is important to obtain the most accurate value for Z_{OM}. This roughness length has the greatest impact on wind speed and ABL height forecasts as explained statistically.

Further studies will include using wind speed wind direction data for an entire season (winter, spring) and extending the area to include coastal locations such as Brownsville, Texas, Tampa, Florida, and Miami, Florida to ascertain the impact of a calculated roughness length. This type of study should also be done over bodies of water. However, model data, such as the *Eta* model or Rapid Updated Cycle (*RUC*), must be used to obtain the observed winds. These studies should also be extended to mesoscale and global models. Multiple regression techniques comparing the calculated roughness lengths of the aforementioned locations can also be done to determine effects of roughness length on model results for both coastal locations and inland locations, separately.

Acknowledgements

Prof. J. B. Elsner of the Florida State University is acknowledged for providing information about statistical approaches used in this paper. Jeremy Grist is thanked for revising this manuscript. Mr. Ken Gould of National Weather Service (NWS) of Tallahassee provided the necessary upper-air data set used in this investigation. We appreciate him in this manner. The support of NCAR for use of their data archive is also acknowledged. We also gratefully acknowledge the interesting comments made by reviewers, which significantly improved the quality of this paper. This work was partially sponsored by the U.S. Air Force of Scientific Research under contract number F19628-93-K-0006.

REFERENCES

André, J. C., and L. Mahrt, 1982. The nocturnal surface inversion and influence of clear air radiative cooling. *J. Atmos. Sci.*, **39**, 864-878.

Arya, S. P. S., 1975. Geostrophic drag and heat transfer relations for the atmospheric boundary layer. *Quart. J. Roy. Meteor. Soc.*, **101**, 147-161.

Beljaars, A. C. M., A. A. M. Holtslag, 1991. Flux parameterization over land surfaces for atmospheric models. *J. Appl. Meteor.*, **30**, 327-341.

Brutsaert, W., 1982. *Evaporation into the atmosphere*, D. Reidel Publ. Co., 299 pp.

Businger, J. A., J. C. Wyngaard, Y. Izumi, and E. F. Bradley, 1971. Flux-profile relationships in the atmospheric surface layer. *J. Atmos. Sci.*, **28**, 181-189.

Clapp, R. B., and G. M. Hornberger, 1978. Empirical equations for some soil hydraulic properties. *Water Resour. Res.*, **14**, 601-604.

Deardorff, J. W., 1972. Parameterization of the planetary boundary layer for use in general circulation models. *Mon. Wea. Rev.*, **100**, 93-106.

Garratt, J. R., 1978. Transfer characteristics for a heterogeneous surface of large aerodynamic roughness. *Quart. J. Roy. Meteor. Soc.*, **104**, 491-502.

Garratt, J. R., and R. A. Pielke, 1989. On the sensitivity of mesoscale models to surface-layer parameterization constants. *Bound. -Layer Meteor.*, **48**, 377-387.

Holtslag, A. A. M., 1987. Surface fluxes, and boundary-layer scaling: Model and applications. KNMI Sci. Rep., 87-02.

Holtslag, A. A. M., and M. Ek, 1996. Simulation of surface fluxes and boundary layer development over the pine forest in HAPEX-MOBILHY. *J. Appl. Meteor.*, **35**, 202-213.

Kara, A. B., 1996a. Analysis of boundary layer structure over and around the Gulf of Mexico. Master thesis, Department of Meteorology, The Florida State University, 78 pp. [Available from Department of Meteorology, Florida State University, 32306-4520, Tallahassee, FL, USA.]

Kara, A. B., 1996b. A user's guide to FSU1DPBL model. Department of Meteorology, The Florida State University, 70 pp. [Available from Department of Meteorology, Florida State University, 32306-4520, Tallahassee, FL, USA.]

Kara, A. B., J. B. Elsner, and P. H. Ruscher, 1998. Physical mechanism for the Tallahassee, Florida minimum temperature anomaly. *J. Appl. Meteor.*, **37**, 101-113.

Kasten, F., and G. Czeplak, 1980. Solar and terrestrial radiation dependent on the amount and type of cloud. *Solar energy*, **24**, 177-189.

Louis J. -F, M. Tiedtke, and J. F. Geleyn, 1982. A short history of the operational PBL Parameterization of ECMWF. Workshop on planetary boundary layer parameterization, European Centre for Medium Range Weather Forecasts, Shinfield Park, Reading, Berks, U.K.

Mahrt, L., and H. -L. Pan, 1984. A two-layer model of soil hydrology. *Bound. -Layer Meteor.*, **29**, 1-20.

Mahrt, L., 1987. Grid-Averaged surface fluxes. *Mon. Wea. Rev.*, **115**, 1550-1560.

Murphy, A. H., 1995. The coefficients of correlation and determination as measures of performance in forecast verification. *Wea. Forecasting*, **10**, 681-688.

Nieuwstadt, F. T. M., and A. G. M. Driedonks, 1979. The nocturnal boundary layer: A case study compared with model calculations. *J. Appl. Meteor.*, **18**, 1397-1405.

O'Brien, J. J., 1970. A note on the vertical structure of the eddy exchange coefficient in the planetary boundary layer. *J. Atmos. Sci.*, **27**, 1213-1215.

Pan, H. -L, and L. Mahrt, 1987. Interaction between soil hydrology and boundary layer development. *Bound. -Layer Meteor.*, **38**, 185-202.

Satterlund, D. R., 1979. Improved equation for estimating long-wave radition from the atmosphere. *Water Resour. Res.*, **15**, 1649-1650.

Stull, R. B., 1983. *An Introduction to Boundary Layer Meteorology.* Kluwer Academic Publishers, 666 pp.

Troen, I., and L. Mahrt, 1986. A simple model of the atmospheric boundary layer model. Sensitivity to surface evaporation. *Bound. -Layer Meteor.*, **37**, 129-148.

Wieringa, J., 1992. Updating the Davenport roughness classification. *J. Wind Eng. Industr. Aerodyn.*, **41**, 357-368.

Zhang, D., and R. A. Anthes, 1982. A high-resolution model of the planetary boundary layer-Sensivity tests and comparisons with SESAME-79 data. *J. Appl. Meteor.*, **21**, 1594-1609.